International Journal of Innovative Research & Growth
A Peer Reviewed Journal
ISSN: 2455-1848
Journal homepage: http://www.ijirg.com/ijirg/
Volume: 11 Issue: 2, April 2022

H-CMEs and solar wind plasma disturbances in relation to intense geomagnetic storms during the period of 2014-2017

Varinder Pandey[1], Saket Kumar[2*], Dolly Ochani[3], P. L. Verma[4]
[1,2,3]Research Scholar, APS University, M.P., India
[4]Department of Physics Govt. Vivekanand P. G. College Maihar, Satna, M.P., India
E-mail: saket301190@gmail.com
* Corresponding Author

Article Info
Received 28 March 2022
Received in revised form 14 April 2022
Accepted for publication 20 April 2022
DOI: 10.26671/IJIRG.2022.2.11.102

Citation:
Pandey, V., Kumar, S., Ochani, D., Verma, P. L. (2022). H-CMEs and solar wind plasma disturbances in relation to intense geomagnetic storms during the period of 2014-2017. *Int J Innovat Res Growth*, 11, 28-34.

Abstract
We have studied intense geomagnetic storms magnitude (≤-100nT) observed between 2014 and 2017 with coronal mass ejections, hard X-ray solar flaresand disturbances in solar wind plasma parameters. We have observed that majority of the of intense geomagnetic storms, associated Hard X-Ray solar flares. It is observed that all the intense geomagnetic storms are Hard X-Ray solar flares of different categories. The association rates X-Class, M-Class, C-Class and B-Class X-ray solar flare are:X-Class -9.0%, M-Class-54.54%, C-Class -18.18%, B-Class -18.18% respectively. Intense geomagnetic storms which are associated with halo and partial halo coronal mass ejection (CMEs) are related to hard X-ray solar flares of different categories. It is also observed that these intense geomagnetic are associated with disturbances in solar wind plasma parameters. Positive correlation with correlation coefficient 0.71 has been found between the magnitude of intense geomagnetic storms and the peak value of associated disturbances in interplanetary magnetic fields (IMFB), 0.49between the magnitude of intense geomagnetic storms and the peak value of associated disturbances in southward component in interplanetary magnetic fields (IMF Bz), 0.79between the magnitude of intense geomagnetic storms and the peak value of associated disturbances in solar wind plasma pressure (SWP) . We have concluded that coronal mass ejections associated with hard X-ray solar flare are mainly responsible to cause intense geomagnetic storms.
Keywords:- Intense geomagnetic storms, Interplanetary magnetic fields, Southward component of interplanetary magnetic fields, solar wind plasma pressure, Coronal mass ejection (CMEs), HCMEs.

1. Introduction

The geo-spheric atmosphere is highly exaggerated by the solar active regions accompanying solar features and interplanetary parameters such as solar flare (SFs), active prominences disappearing filaments (APDFs), coronal holes, coronal mass ejections (CMEs), radio bursts, interplanetary shocks and turbulences in solar wind plasma parameters. The active regions and related major classes of solar activity tend to track the sunspot number during the cycle, including- radio burst, calcium plages, solar flares, filaments, and coronal mass ejections (CMEs) (Webb and Howard (1994). This activity is transmitted to earth through the solar corona and its expansion into the heliosphere as the solar wind. Among all these solar features radio bursts, solar flares, and coronal mass ejections are the most energetic solar events in the heliosphere and are widely recognized as being responsible for the production of large disturbances in the solar wind, transient interplanetary shocks, and geomagnetic disturbances in geomagnetic field of the magnetosphere. From the result of the investigation, it has now been clear that geomagnetic perturbations in the magnetosphere are produced by helio-spheric magnetic fields and solar wind plasma streams related to the active regions, disappearing filaments and prominences, solar flares, evolving active regions, and coronal holes (CH), helio-spheric current sheet, (HCS). It is generally believed that long intervals of enhanced southward interplanetary magnetic field (IMF) and the high solar wind speed are the primary causes of intense geomagnetic disturbances in the geomagnetic field of the magnetosphere and that the solar sources of such geoeffective solar wind structures are usually CMEs (Webb et al. 2001). However, not all Earth-directed CMEs can produce geomagnetic storms in the magnetosphere. The properties of the earth-directed CMEs, such as the internal structure of the magnetic field, may determine whether or not a geomagnetic storm subsequently occurs (Burton et al. 1975, Cane et al.2000). From the results of the past three decades, it is confirmed that CMEs are large-scale magnetized plasma structures originating from closed magnetic field regions the sun: active regions, filament regions, active region complexes, and trans equatorial interconnecting regions (Gopalswamy 2006) and drive solar wind (SW) disturbances in terms of the magnetic field, speed

and density, which in turn cause magnetic disturbance in the magnetosphere (Zhang, et al 2003). It has been established by now that geomagnetic storms occur when the southward component of interplanetary magnetic field eld (IMF), *Bz*, impinges upon the Earth's magnetosphere and reconnects (Gopalswamy, 2002). Several statistical observational studies have been done to investigate the properties of solar flares and/or CMEs. By focusing on flare occurrence, Bobra & Couvidat (2015) showed that a few parameters (total unsigned current helicity, total magnitude of Lorentz force, and total photo-spheric magnetic free energy density) are more relevant to the occurrence of solar flares than other parameters (mean photo-spheric magnetic free energy and mean current helicity). Zhang & Liu (2015) indicated that the rise time of the soft-X-ray flux of a flare is approximately half of the decay time, and the rise and decay times increase with variations in the peak flux of the soft X-ray. Regarding CMEs, Yashiro et al. (2006) investigated the frequency distributions in the energy of solar flares and found that the power law indices of the frequency distributions for flares without CMEs are steeper than those for flares with CMEs. According to Toriumi et al. (2017), if the area of flare ribbons normalized by the sunspot area is large, solar flares tend to be accompanied by CMEs. Another important observational characteristic of solar flares is the shape of the magnetic field lines in the corona. Since the plasmas in the corona are frozen to the magnetic field lines, the loop-like structure, which can be seen through soft X-ray or extreme ultraviolet (EUV) observations, reflects the structure of the magnetic field lines. Verma et al, (2009) have studied geomagnetic storms Dst < - 50nT observed during the period of 1997-2006, with halo and partial halo coronal mass ejections associated with X-ray solar flares of different categories and concluded that they have concluded that majority of the observed geomagnetic storms are found that halo and partial halo CMEs associated with X ray solar flares are most potential candidates for production of geomagnetic storms. Michalek, G.et al (2006) have concluded that halo coronal mass ejections (HCMEs) originating from regions close to the centre of the sun are likely to be geoeffective. They have showed that, only fast halo CMEs (with space velocities higher than ~1000 km/s) and originating from the Western Hemisphere close to the solar centre could cause intense geomagnetic storms. Gopalswamy (2009) has studied the role of halo and partial halo CMEs in producing geomagnetic storms. He has reviewed the results obtained by previous investigators and concluded that the generation of geomagnetic storms rates can be readily explained by the different definition of halo CMEs used by different authors. Partial halos are less energetic and generally originate far from the disk centre, so most of them behave similar to the non-geo-effective CMEs and hence most of the partial halo CMEs may not produce geomagnetic storms. He has inferred that halo CMEs originating close to the disk centre or very much effective in producing geomagnetic storms. Since coronal plasmas are heated to 10–20 MK during solar flares, the characteristics of solar flares are often identified through X-ray observations (e.g., Benz 2017 and references therein). The magnitude of a solar flare is usually defined by the peak flux of the soft-X-ray measured by the Geostationary Operational Environmental Satellite (GOES) and classified into several classes (A, B, C, M, and X). In this investigation, we have studied intense geomagnetic storms magnitude (≤-100nT) observed between 2014 and 2017 with coronal mass ejections, hard X-ray solar flares and disturbances in solar wind plasma parameters. In this study, we use the linear CME speeds to further explore their geomagnetic activity. One obvious reason to use this parameter is that fast CMEs are very often associated with strong geomagnetic storms (Gopalswamy, 2010).

This paper is organized as follows. The observations and data selection are described in Section 2, and the analysis is explained in Section 3. Section 4 presents the results and final conclusion in Section 5.

2. Data Selection and Observations

Table1- Instance geo-magnetic storms and associated disturbances in solar wind plasma parameters for the period of 2014-2017.

Intense Geomagnetic storms			Disturbances in IMF B			Disturbances in IMF Bz (GSE)			Disturbances in Solar Wind Plasma Pressure		
year	on set time	Magnitude Dst (nT)	Disturbance Start Time	Disturbances Peak Value	Disturbance Magnitude	Disturbance Start Time	Disturbances Peak Value	Disturbance Magnitude	Disturbance start time	Disturbance Peak Value	Disturbance Magnitude
2014	49(13)	-119	49(15)	18.6	14.2	49(17)	-12.9	-12.3	50(1)	688	300
2015	7(6)	-106	17(2)	21.6	15.8	7(2)	-17.4	-16.8	8(6)	508	75
2015	76(7)	-217	76(3)	31.5	23.7	76(9)	-18.1	-13.7	76(3)	666	254
2015	173(11)	-206	173(5)	25.6	16.9	173(17)	-26.3	-24	172(11)	742	463
2015	274(17)	-116	279(5)	20.8	16.4	280(11)	-11.2	-10.2	279(14)	775	398
2015	354(4)	-161	354(11)	19.5	11.9	354(11)	-18.7	-11.4	355(19)	457	83
2016	4(4)	-102	365(0)	16.9	11.4	365(19)	-15.8	-7.7	1(18)	490	81
2016	66(16)	-102	65(16)	20.1	16.6	66(15)	-11.9	-5.4	65(20)	590	239
2016	287(6)	-112	287(4)	24.1	19.9	287(3)	-20.8	-19.5	258(12)	717	363
2017	147(14)	-131	147(9)	22.8	20.7	147(20)	-19.5	-19.4	147(10)	401	105
2017	250(21)	-123	249(20)	13.9	11.6	250(20)	-24.2	-23.5	249(20)	817	417

In table 1 investigation of hourly Dst indices of geomagnetic field have been used over the period 2014 through 2017 to determine onset time, maximum depression time, the magnitude of intense geomagnetic storms. This data has been taken from the NSSDC Omni web data system (http;//omniweb.gsfc.nasa.gov/form/dxi.html)). Which has been created in late 1994 for enhanced access to the near-earth solar wind, magnetic field, and plasma data of Omni data set, which consists of one-hour resolution near the earth, solar wind magnetic field and plasma data, energetic proton fluxes and geomagnetic and solar activity indices? To determine disturbances in solar wind plasma parameters, hourly data of solar wind plasma pressure and interplanetary magnetic field, the southward component of interplanetary magnetic fields has been used and these data have also been taken from Omni web data (http;//omniweb.gsfc.nasa.gov/form/dxi.html).

Table 2 – Type of CMEs, Solar flares and associated disturbances in solar wind plasma parameters for the period of 2014-2017.

Date	Onset time in dd(hh)	Class of solar flares	Date	Time	Type of CMEs H/P
18.02.2014	49(13)	M	16.02.2014	10:00:05	HALO
07.01.2015	7(6)	M	NA	NA	NA
17.03.2015	76(7)	M	15.03.2015	01:48:05	HALO
22.06.2015	173(11)	M	21.06.2015	02:36:05	HALO
01.10.2015	274(17)	M	30-09-2015	00:00:00	P.H
20.12.2015	354(4)	C	19.12.2015	13:25:47	P.H
04.01.2016	4(4)	M	01.01.2016	23:24:04	HALO
06.03.2016	66(16)	C	NA	NA	NA
13.10.2016	287(6)	B	10.10.2016	08:36:05	P.H
27.05.2017	147(14)	B	23.05.2017	05:00:06	P.H
07.09.2017	250(21)	X	06.09.2017	12:24:05	HALO

In table 2 investigation of hourly Dst indices of geomagnetic field have been used over the period 2014 through 2017 to determine date, onset time, Type of CMEs, type of solar flares. The data of coronal mass ejections (CMEs) have been taken from SOHO – large-angle spectrometric, coronagraph (SOHO / LASCO), and extreme ultraviolet imaging telescope (SOHO/EIT) data. The data of X-ray solar flares are taken from STP solar data (http://www.ngdc.noaa.gov/stp/solar/solardataservices.html).

3. Analysis

This study uses statistical method association and correlation for data analysis of the observed intense geomagnetic storms with disturbances in solar wind plasma parameters. Statistical method correlation has been used to see how the magnitude of intense geomagnetic storms is correlated with disturbances in solar wind plasma parameters.

1. From the data analysis of intense geomagnetic storms and associated disturbances in a southward component of interplanetary magnetic fields (IMF Bz) given in Table and Figure 1,2 it is observed that all the intense geomagnetic storms are associated with disturbances in the southward component of interplanetary magnetic fields (IMF Bz) with lowest peak value -11.2 nT to highest peak value -26.3 nT and lowest magnitude -5.4 nT to highest magnitude -23.5 nT. Most of the intense geomagnetic storms of higher magnitudes are associated with relatively higher peak value disturbances in IMF Bz. The trend line of scatter plot between the magnitude of intense geomagnetic storms and the peak value of IMF Bz given in Figure 1 and magnitude of intense geomagnetic storms and magnitude of disturbances in IMF Bz given in Figure 2 shows a strong positive correlation. A large positive correlation with correlation coefficient 0.49 between peak values of disturbances in IMF Bz and magnitude of intense geomagnetic storms and between the magnitude of disturbances in IMF Bz and magnitude of intense geomagnetic storms have been obtained by statistical methods.

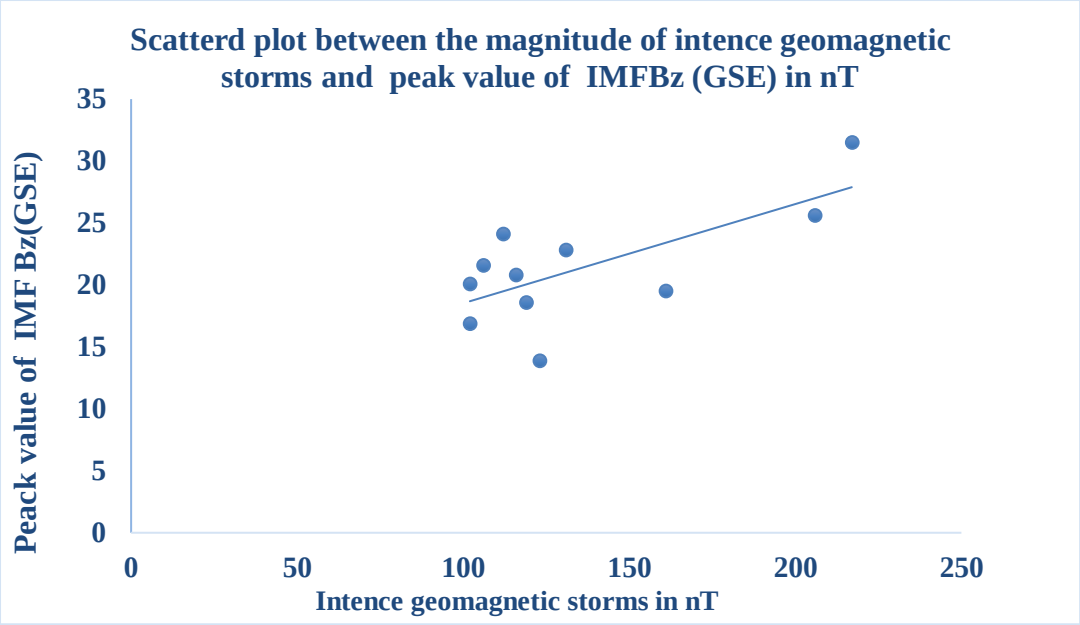

Figure-1 Shows scatter plot between the magnitude of intense geo-magnetic and the magnitude of disturbances in IMF Bz (GSE).

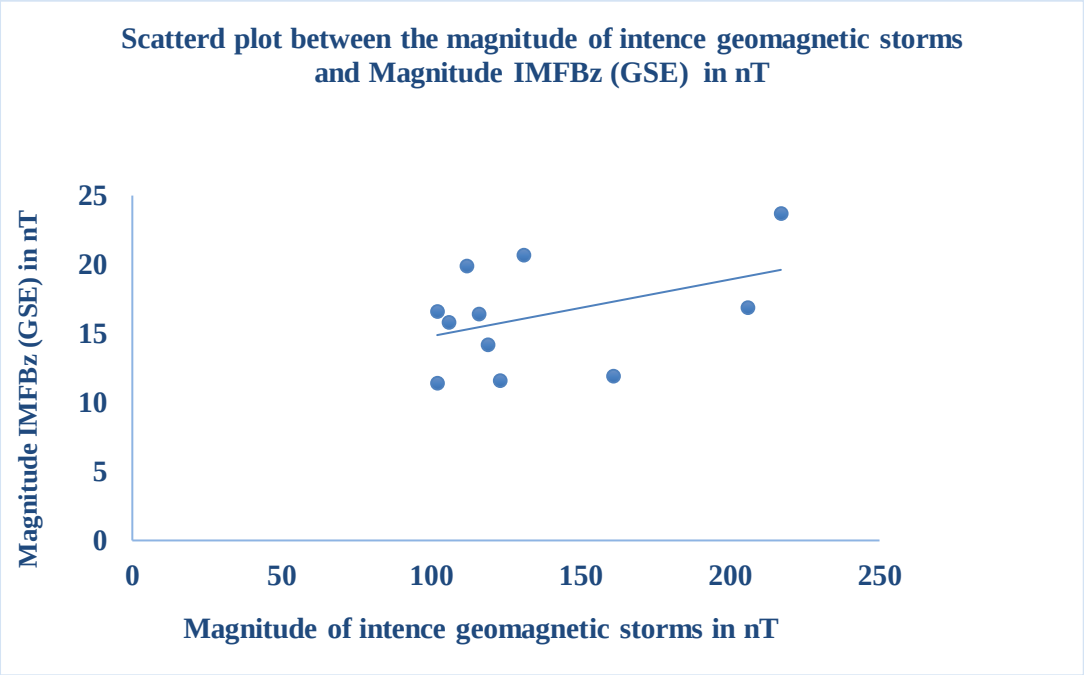

Figure-2 Shows scatter plot between the magnitude of intense geo-magnetic storms and the peak value of disturbances in IMF Bz (GSE).

2- The results of the data analysis of intense geomagnetic storms and associated disturbances in interplanetary magnetic fields (IMFB) given in Table and Figure 3 shows that all the intense geomagnetic storms are associated with disturbances in interplanetary magnetic fields (IMFB) with the lowest peak value 13.9 nT, and highest peak value 31.5nT and lowest magnitude 11.5 nT and highest magnitude 23.7 nT. It is also seen that the disturbances in IMFB following the onset time of intense geomagnetic storms. The trend line of the scatter plot between the magnitude of intense geomagnetic storms and the peak value of IMFB (Figure 3) and magnitude of intense geomagnetic storms and magnitude of disturbances in IMFB given in Figure 3 shows a strong positive correlation. positive correlation with correlation coefficient 0. 71 has been determined between magnitude of intense geomagnetic storms peak value of associated disturbances in interplanetary magnetic fields (IMFB) and magnitude of intense geomagnetic storms have been by statistical methods.

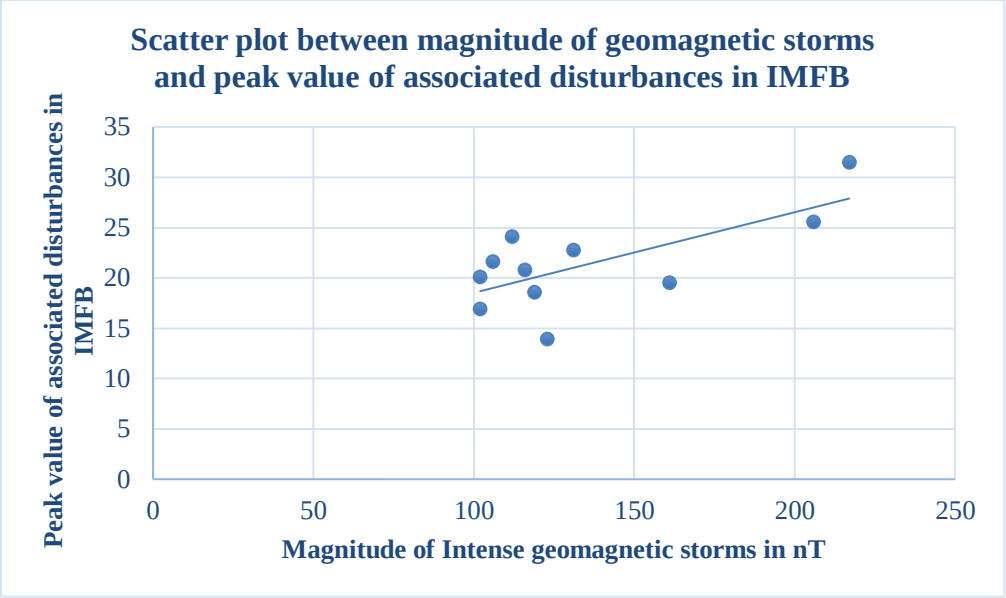

Figure-3 Shows Scatter plot between magnitude of geomagnetic storms and peak value of associated disturbances in IMFB (GSE).

3- From the data analysis of intense geomagnetic storms and associated disturbances in solar wind plasma pressure observed during the period of 2014-2017. In figure 4 it is determined that all the all the intense geomagnetic storms are associated with disturbances in solar wind plasma pressure. Positive correlation with correlation coefficient 0.79has been determined between magnitude of intense geomagnetic storms peak value of associated disturbances in solar wind plasma pressure.

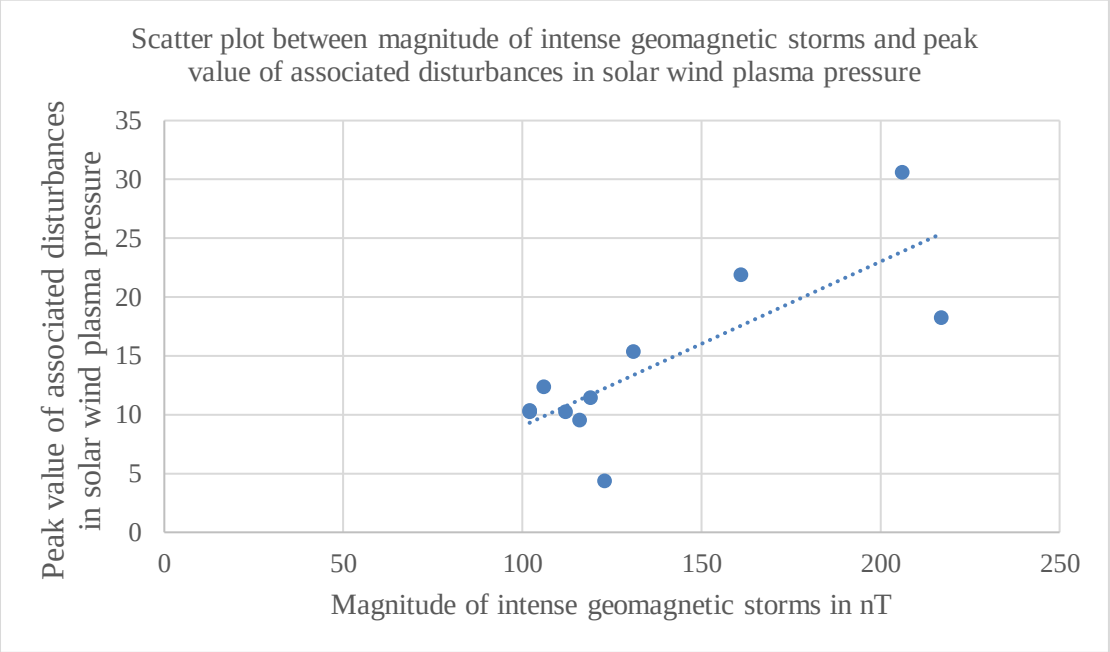

Figure-4 Shows Scatter plot between magnitude of intense geomagnetic storms and peak value of associated disturbances in solar wind plasma pressure.

4. The data analysis of intense geomagnetic storms associated Hard X-Ray solar flares in figure 5. It is observed that all the intense geomagnetic storms are Hard X-Ray solar flares of different categories. The association rates X-Class, M-Class, C-Class and B-Class X-ray solar flare are: X-Class -9.0%, M-Class-54.54%, C-Class -18.18%, B-Class -18.18% respectively.

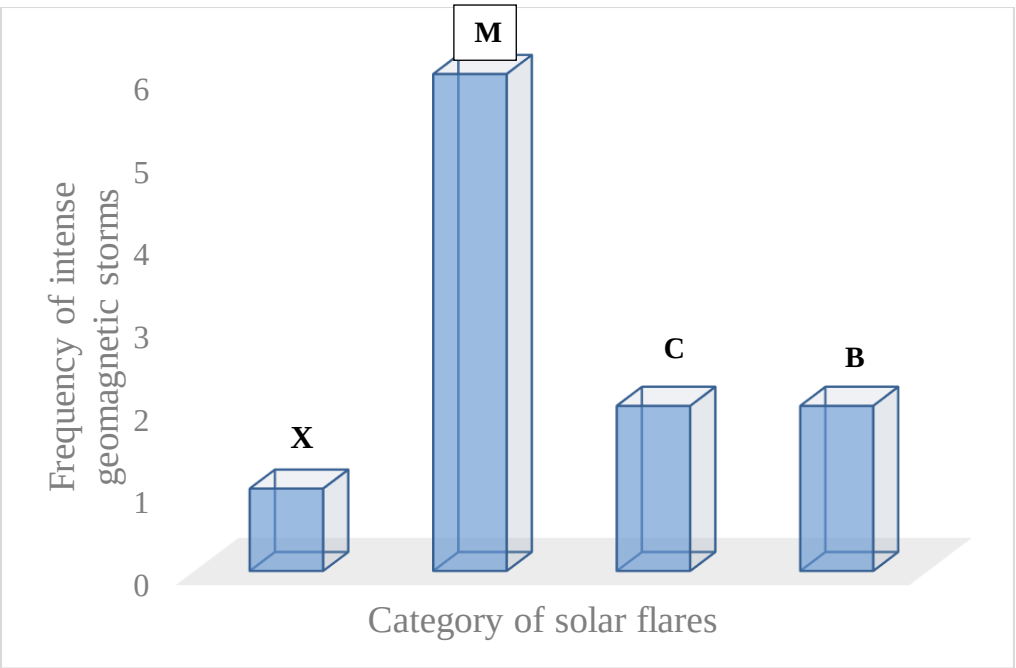

Figure-5 Bar diagram between frequency of intense geomagnetic storms and category of solar flares.

4. Results

Our analysis showed that all analyzed data sets have significant relationships with each other. This study based on the comparison of instance geomagnetic storms magnitude (≤-100nT) observed between 2014 and 2017 with coronal mass ejections (CMEs), hard X-ray solar flares and disturbances in solar wind plasma parameters (IMFB, IMF Bz).We summarize the main findings of this study as follows: We have observed that the data analysis of intense geomagnetic storms, associated Hard X-Ray solar flares in figure 5. It is observed that all the intense geomagnetic storms are Hard X-Ray solar flares of different categories. The association rates X-Class, M-Class, C-Class and B-Class X-ray solar flare are: X-Class -9.0%, M-Class-54.54%, C-Class -18.18%, B-Class -18.18% respectively. Intense geomagnetic storms which are associated with halo and partial halo coronal mass ejection (CMEs) are related to hard X-ray solar flares of different categories. Further it is also observed that these intense geomagnetic are associated with disturbances in solar wind plasma parameters. Positive correlation with correlation coefficient 0.71 has been found between the magnitude of intense geomagnetic storms and the peak value of associated disturbances in interplanetary magnetic fields (IMFB). Positive correlation with correlation 0.49 has been determined between the magnitude of intense geomagnetic storms and the peak value of associated disturbances in southward component in interplanetary magnetic fields (IMF Bz). Positive correlation with correlation 0.79 has been determined between the magnitude of intense geomagnetic storms and the peak value of associated disturbances in solar wind plasma pressure (SWP).

5. Conclusions

We performed statistical analyses to compare the dependence among the parameters of solar flares existence, flare class, duration, decay time, rise time, CME speeds, and CME type, based on two analyses: linear-correlation analysis method and graphical representation method. Our statistical analysis concluded that coronal mass ejections (CMEs) associated with hard X-ray solar flares are mainly responsible to generate intense geomagnetic storms.

Conflict of Interest

In this manuscript the authors declare that there is no conflict of interest.

References

i. Archontis, V., Hood, A. W., Savcheva, A., Golub, L., and Deluca, E. (2009). On the structure and evolution of complexity in sigmoid: a flux emergence model. *ApJ*, 691, 1276.
ii. Bobra, M. G., and Couvidat, S. (2015). Solar flare prediction using sdo/hmi vector magnetic field data with a machine-learning algorithm. *ApJ*, 798, 135.
iii. Burton, R. K., McPherron, R. L., and Russell, C. T. (1975). An empirical relationship between interplanetary conditions and Dst. *J. Geophys. Res.*, 80, 4204.
iv. Benz, A. O. (2017). Flare observations. *LRSP*, 14, 2.
v. Cheng, X., Ding, M. D., Zhang, J., et al. (2014). Formation of double- decker magnetic flux rope in the sigmoidal solar activity region 11520. *ApJ*, 789, 93.
vi. Cane, H. V., Richardson, I. G., and St. Cyr, O. C. (2000). Coronal mass ejections, interplanetary ejecta and geomagnetic storms. *Geophys. Res. Lett.*, 27, 3591.

vii. Gopalswamy, N. (2002). Coronal mass ejections and their geospace consequences, in *Proc. of the Silver Jubilee Symposium of the Udaipur Solar Observatory*, India.
viii. Gopalswamy, N. (2006). Coronal mass ejections of solar cycle 23. *J. Astrophys. Astron.*, 27, 243.
ix. Gopalswamy N. (2009). Halo coronal mass ejections and geomagnetic storms. *Letter Earth Planets Space*, 61, 1–3.
x. Gopalswamy, N., Akiyama, S., Yashiro, S., and Makela, P. (2010). Magnetic Coupling between the Interior and Atmosphere of the Sun in Astrophys. *Sp. Sci. Proc.*, ed. S. S. Hasan & R. J. Rutten (Berlin: Springer) 289.
xi. Liu, C., Lee, J., Yurchyshyn, V., et al. (2007). The eruption from a sigmoidal solar activity region on 2005 may 13. *ApJ*, 669, 1372.
xii. Michalek, G., Gopalswamy, N., Lara, A., and Yashiro (2006). Properties and geo-effectiveness of halo coronal mass ejections. Space. *Weather*, 4.
xiii. Rust, D. M., and Kumar, A. (1996). Evidence for helically kinked magnetic flux ropes in solar eruptions. *ApJL*, 464, L199.
xiv. Toriumi, S., Schrijver, C. J., Harra, L. K., Hudson, H., and Nagashima, K. (2017). Electric current neutralization in solar active regions and its relation to eruptive activity. *ApJ*, 834, 56.
xv. Verma, P. L., Tripathi, A .K. and Sharma, S. (2009). Coronal Mass Ejections, Interplanetary shocks in relation with forbush decreases associated with intense geomagnetic storms. *J. Plasma Fusion Res. SERIES*, 8, 221-225.
xvi. Webb, D. F. and Howard, R. A. (1994). The solar cycle variation of coronal mass ejections and the solar wind mass flux. *J. Geophys. Res.*, 99, 4201.
xvii. Webb, D. F., Crooker, N. U., Plunkett, S. P., and St. Cyr, O. C. (2001). Forecasting helio-spheric structure using the solar mass ejection imager (SMEI) in Geophysics Monograph Ser. 125, Space Weather, ed. Song, P., Siscoe, G., & Singer, H., 123.
xviii. Yashiro, S., Gopalswamy, N., Michalek, G., St., et al. (2004). A catalog of white light coronal mass ejections observed by the SOHO spacecraft 2004. *JGRA*, 109, A07105.
xix. Zhang, J., Dere, K. P., Howard, R. A., Kundu, M. R., and White, S. M. (2001). On the temporal relationship between coronal mass ejections and flares. *ApJ*, 559, 452.
xx. Zhang, J K P Dere, Howard, R. A. and Bothmer, V. (2003). Identification of Solar Sources of Major Geomagnetic Storms between 1996 and 2000. *The Astrophys. J.*, 582, 520.
xxi. Zhang, P., and Liu, S.-M. (2015). Statistical Relation between Solar Flares and Coronal Mass Ejections with Respect to Sigmoidal Structures in Active Regions. *ChA&A*, 39, 330.